Development of a Floating Element for the Measurement of Surface Shear Stress

M. Acharya,* J. Bornstein,* M. P. Escudier,† and V. Vokurka‡
Brown Boveri Research Center, Baden, Switzerland

A floating-element instrument has been built based upon a precision galvanometer as the essential balance mechanism. The coil current necessary to maintain the element in its null position is directly proportional to the imposed force and is controlled by a feedback loop in which a key component is a fiber-optic scanner. A series of experiments performed in smooth-wall turbulent boundary layers confirms that the principal uncertainty in determining surface shear stress using the instrument arises from the buoyancy force due to the pressure variation within the gap surrounding the element. It is shown that, for a range of element geometries tested, the flow in the gap does not influence the boundary layer and the buoyancy force is adequately modeled by the expression $ft(\mathrm{d}p/\mathrm{d}x)\pi D^2/4$. The value of f for elements with t/g greater than about 40 is found to be 0.43, close to the value 0.5 for a linear variation of gap pressure. For smaller values of t/g, the value of f is also smaller and less well defined. With this model for the buoyancy force, measurement accuracy is better than 5% for surface shear forces greater than about 300 μN.

Nomenclature

c_f = skin-friction coefficient, $=\tau_s/\frac{1}{2}\rho u_\infty^2$
D = diameter of floating element
d = diameter of Preston tube
d^+ = nondimensional Preston tube diameter, $=u_\tau d/\upsilon$
F_M = total force indicated by instrument
F_τ = wall shear force
ΔF = residual or buoyancy force
f = proportionality factor in buoyancy-force model
g = gap width
L = moment arm
p = local static pressure at surface
p_H = static pressure in instrument housing
p_0 = static pressure at element center ($x=0$)
p_G = static pressure within gap
p^+ = pressure gradient parameter, $=\upsilon/(\rho u_\tau^3)\,\mathrm{d}p/\mathrm{d}x$
Δp_0 = pressure difference, $=p_H-p_0$
t = thickness of floating-element lip
u = velocity
u_∞ = freestream velocity
u_τ = shear velocity, $=\sqrt{\tau_s/\rho}$
x = streamwise coordinate
x_0 = offset from pivot point
y = distance from surface
z = protrusion or recession of element relative to surface
z^+ = nondimensional protrusion or recession of element, $=zu_\tau/\upsilon$
δ = boundary-layer thickness
ϵ = residual error in floating-element measurement
θ = angular position within gap around floating element
ρ = fluid density
τ_s = wall shear stress
υ = kinematic viscosity of fluid

Introduction

THE quantity of principal interest in many aerodynamic problems is the surface shear stress τ_s. For a few simple situations, τ_s can be either calculated theoretically or inferred from measurements of the mean velocity distribution in the vicinity of the surface. The graphical method of Clauser[1] is a widely used example of the latter approach for a turbulent boundary layer developing on a smooth surface. However, for only slightly more complex situations, e.g., the flow over a rough surface, Clauser's method may be grossly inaccurate[2] and other indirect methods which rely upon similarity principles, such as Preston tubes and calibrated heat-transfer gages, are of limited applicability. For most applications, a measurement of τ_s that is independent of such similarity assumptions is the only one which can be considered free from objections of principle. Flow over a rough surface and transitional boundary layers are only two examples of flows of considerable engineering significance where few, if any, reliable measurements of τ_s have been reported due to the lack of a suitable instrument.

There have been numerous attempts to develop a floating-element device for such measurements, but these have not been completely successful primarily because the element is subject to a number of forces, and under some operating conditions τ_s must be obtained as a small difference between large quantities, not all of which can be estimated accurately. A comprehensive review of floating-element skin-friction balances was made by Winter,[3] since which a few new reports have appeared, including those of Schetz and Nerney,[4] Voisinet,[5] and Karlsson[6] for rough-surface measurements, Frei and Thomann[7] for severe pressure gradients in a cylindrical channel, and Tennant et al.[8] for three-dimensional flows.

In an attempt to analyze the so-called "secondary" forces which act on a floating element, Allen[9,10] discusses the importance of gap width, element protrusion or depression (misalignment), and lip thickness. Allen shows that small gaps are more sensitive to misalignment than larger ones, and that a parallel linkage (to absorb off-center normal forces) is superior to a single pivot. Although Allen's work is helpful in assessing the relative importance of the influences mentioned, no comparisons were made with independent measurements. Also, all measurements were made in zero-pressure gradient, although Allen is brought indirectly to address the influence of a longitudinal pressure gradient in discussing the effect of misalignment, which produces a nonuniform pressure over the face of the element.

Detailed consideration of the behavior of a floating element in an adverse pressure gradient was made by Brown and Joubert,[11] who investigated indirectly the forces due both to

Received Oct. 5, 1983; revision received Feb. 6, 1984.

*Research Scientist, Fluid Mechanics Group.
†Group Leader, Fluid Mechanics.
‡Research Scientist, Electronics Group.

the direct effects of a pressure gradient and local distortion of the boundary layer which may be brought about by flow through the gap surrounding the element. The largest discrepancy was found to be about 15% of the shear-stress force (Preston-tube measurements being used as the standard of comparison). Using similarity arguments an empirical correction based upon a correlation with the pressure gradient and the element Reynolds number was shown to reduce this to about 5%.

Everett[12] examined the effects of a favorable pressure gradient on the behavior of a floating element in turbulent channel flow for elements of different lip thicknesses and gap sizes. He concluded that for large thicknesses and small gap widths, the pressure distribution in the gap could be adequately modeled to account for its effect on the floating-element measurement. Although the present work is in basic agreement with Everett's conclusions, it is shown subsequently that they are not well supported by a close examination of his data.

In the present paper the authors report on the development of a floating element and present the results of further efforts to resolve the problem of accounting for secondary forces.

Description of the Floating-Element Instrument

The basic layout of this floating-element design is shown in Fig. 1. The central component (A) is the movement of a precision galvanometer§ which supports the element itself, a disk of 20 mm diameter (B), at the end of an arm which would normally act as a pointer (C). A counterweight (D) allows horizontal positioning of the floating element for calibration, and an arm (E) serves to carry weights for in-situ calibration checks. The movement is attached to an assembly of five aluminium slabs (F-J) which are connected to each other and the baseplate (K) by compression springs (L) and nine differential adjustment screws (M) each of which provides a movement of 50 μm/turn thereby permitting accurate positioning of the element in the surrounding baseplate.

The position of a target (N) on the back of the element is detected by a fiber-optic scanner (O)¶ with a spatial resolution of 0.25 μm. The rotating coil system and optical-position detector operate in a nulling feedback control loop (Fig. 2). The proportional-integral-differential (PID) controller ensures high accuracy and good transient behavior. The coil current I and corresponding control-circuit output voltage V are directly proportional to the imposed force. A low-pass (LP) filter suppresses output-voltage oscillations due to changes in the imposed force; the overall system frequency response is then on the order of 0.5 Hz. The entire floating-element mechanism is enclosed in a sealed housing (P) to which a pressure tap is connected such that the pressure difference Δp_0 across the element can be made either positive or negative. A photograph of the floating element with the housing removed is shown in Fig. 3.

The basic calibration of the instrument is against a precision (0.1%) 100 mg weight hung from the face of the element with the instrument oriented with the arm C and the coil axis in a horizontal plane. The calibration is checked periodically when the element is fully assembled by hanging a range of weights on the shorter arm E. Such checks have revealed negligible departures from linearity—a further consequence of using a standard galvanometer movement.

Although Allen[10] recommends the use of a parallel linkage, the use of a standard galvanometer single-pivot movement was seen as a way of circumventing the many additional problems which would have been introduced by the associated necessity of designing a balance in its entirety. Such movements are readily available with the required range and resolution, inexpensive, and relatively rugged, although care obviously must be exercised in the use of such a sensitive precision instrument. As was stated in the Introduction, the original motivation for the development of a floating element was the need for an instrument to measure τ_s for rough-surface boundary layers. By so simplifying the design, it was realistic to contemplate building a separate unit for each different surface to be investigated. An additional benefit is that it has been possible to produce and individually test several instruments in order to check reproducibility, the influences of geometry, and various modifications made in an effort to identify and possibly eliminate sources of error. The important dimensions of the smooth-surface instruments used for the present investigation are given in Table 1. The length of moment arm L is 35 mm for all instruments.

§Micro-Amperemeter PFF-1, Gossen GmbH, Erlangen, Federal Republic of Germany.

¶Nano-Skan Fiber/Optic Skanner S2005-3, SKAN-A-MATIC Corp., Elbridge, N.Y.

Analytical Considerations

A floating-element device is based upon the principle of measuring the force directly on a small segment of the surface isolated from its surroundings (see Fig. 4). In a general flow situation the steady-state balance of moments exerted on the floating element is modeled as follows:

$$F_M L = F_\tau L - \Delta p_0 \frac{\pi D^2}{4} x_0 + \frac{1}{64}\frac{dp}{dx}\pi D^4 - \frac{1}{2} LD \int_0^t \int_0^{2\pi} p(\theta,z)\cos\theta \, d\theta \, dz \quad (1)$$

where F_M is the force indicated by the instrument and the friction force $F_\tau = \tau_s \pi D^2/4$, τ_s thereby representing an average of the shear stress acting on the element. The second term on the right-hand side of Eq. (1) arises due to the fact that, for the balance movements used, it is possible for the pivot point to be offset by a distance x_0 from a normal to the face of the element passing through its center. The magnitude of x_0 given in Table 1 for each element tested was obtained by varying Δp_0 in a no-flow test, when all other contributions to F_M in Eq. (1) are absent. The results of such a test for instrument 2 are given in Fig. 7. A uniform pressure gradient across the face of the element results in a couple given by the third term on the right-hand side of Eq. (1) (measurements show that the pressure variation across a small element such as that presented herein is indeed closely linear). The last term in Eq. (1) represents the effect of a pressure variation over the element lip. A major difficulty in efforts to develop floating-element devices is in accounting for and modeling this effect, termed the lip, or buoyancy force.

The pressure on the element lip varies both with angular location θ around the gap as well as along the lip thickness. It may reasonably be assumed that the lip pressure varies between the housing pressure p_H and the external pressure, which can be approximated by $p_0 + (D/2)(dp/dx)\cos\theta$. The form of the variation between these values presumably depends upon the magnitudes of the lip thickness and gap width. In spite of

Table 1 Important dimensions of the floating elements

Instrument	t, mm	D, mm	g, mm	t/g	x_0, mm
1	0.6	19.95	0.05	12.0	0.72
2	0.8	19.88	0.03	26.7	0.39
3	0.02	19.89	0.06	0.4	0.92
4	0.2	19.91	0.06	3.6	0.65
5	0.8	19.82	0.08	10.0	0.34
6	2.0	19.87	0.08	25.0	−0.46
7	3.0	19.86	0.07	42.9	1.03
8	6.0	19.87	0.06	100.0	0.00

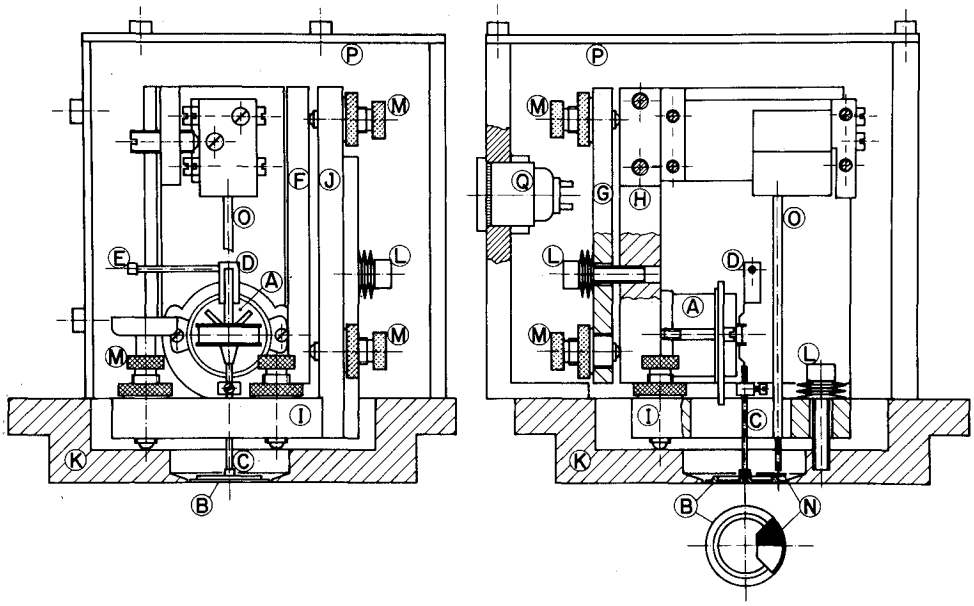

Fig. 1 Design of floating element.

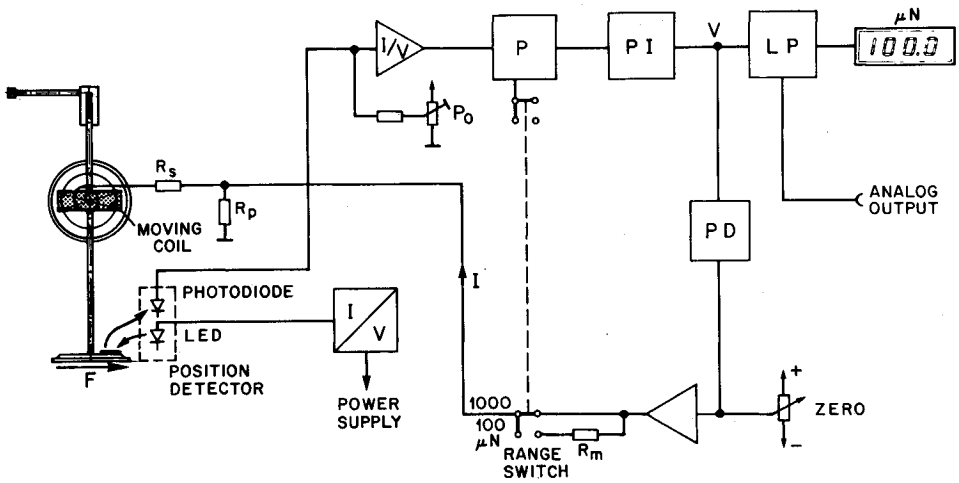

Fig. 2 Schematic of feedback control loop.

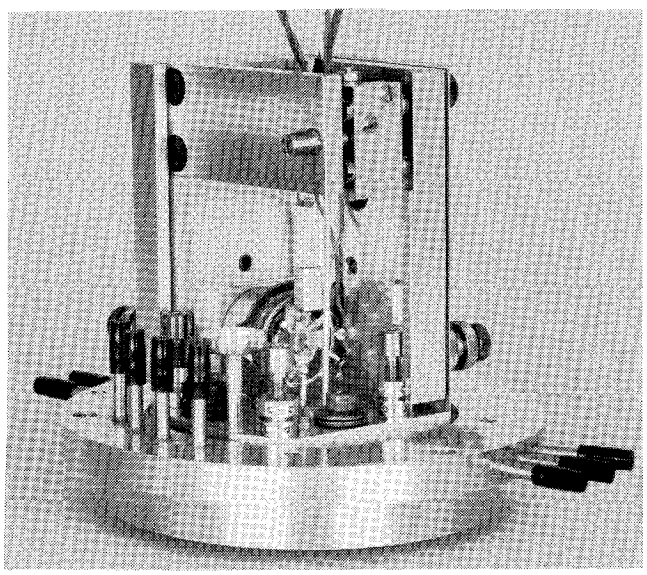

Fig. 3 Floating element with housing removed.

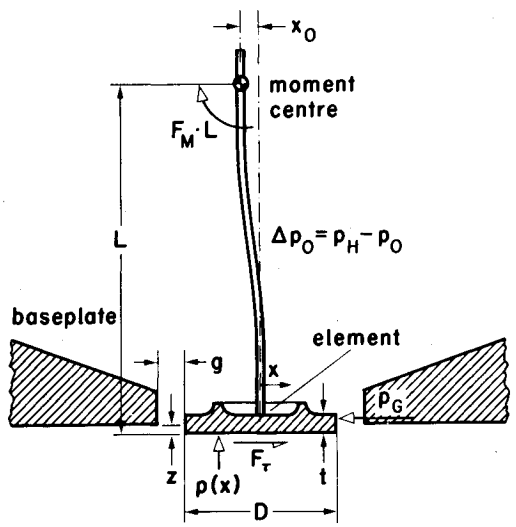

Fig. 4 Floating-element analysis.

the high precision achievable in the machining, assembly, and alignment of the various parts, the gap width varies with angular position. In addition, Eq. (1) assumes time-invariant behavior, whereas during actual operation the element makes continuous excursions about its mean position so that the gap width changes continuously with time. Therefore, it seems worthwhile to examine the applicability of a simple model for the variation of the gap pressure. The assumption of a steady, linear pressure variation along the lip at any azimuthal location leads to the result $ft(\mathrm{d}p/\mathrm{d}x)\pi D^2/4$, with $f=0.5$, for the buoyancy force. This expression was first used by Coles[13] for a rectangular element, and later adopted by Everett[12] and Brown and Joubert[11] for circular elements. As is discussed below, the buoyancy force has been experimentally determined as the difference between the net measured force F_M, and the remaining force contributions on the right-hand side of Eq. (1) as

$$\Delta F \equiv F_M - \left[F_\tau - \frac{\Delta p_0 \pi D^2 x_0}{4L} + \frac{1}{64}\frac{\mathrm{d}p}{\mathrm{d}x}\frac{\pi D^4}{L}\right]$$

Setting $\Delta F = ft(\mathrm{d}p/\mathrm{d}x)\pi D^2/4$ then leads to a value for the factor f.

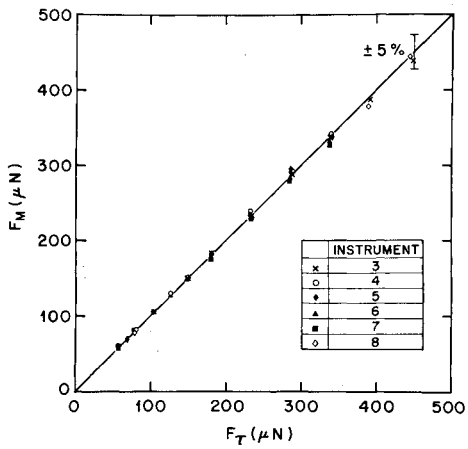

Fig. 5 Comparison of floating-element and Preston-tube data for $\mathrm{d}p/\mathrm{d}x=0$.

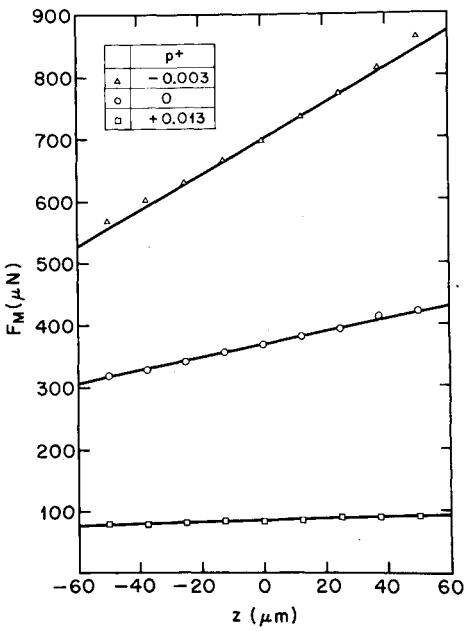

Fig. 6 Influence of misalignment z on indicated force F_M for instrument 5.

Floating-Element Tests

The instruments listed in Table 1 were tested extensively in a Bradshaw-type[14] boundary-layer wind tunnel in which fully developed turubulent boundary layers with variable pressure gradients can be obtained. The test section measures 100×800 mm at the inlet and is 3000 mm long. For the present tests $10<u_\infty<40$ m/s, $-0.007<p^+<0.3$, and the boundary-layer thickness varied typically between 10 and 50 mm.

Our standard of comparison for the wall shear-stress measurements was the Preston tube, the accuracy of which is a function of d^+ and p^+: for instance, Patel[15] shows that for $d^+ \leqq 200$ and $p^+ < 0.01$ the maximum error in the measured shear stress is 3%. Frei and Thomann[7] have extended this result to obtain a set of constant-error contours on a plot of d^+ vs p^+. For the measurements discussed here, the Preston-tube data fall well within the 5% error contour.

Zero Pressure Gradient Tests and Alignment Effects

As shown in Fig. 5, for flows with zero external pressure gradient, our floating elements all yielded values of the shear

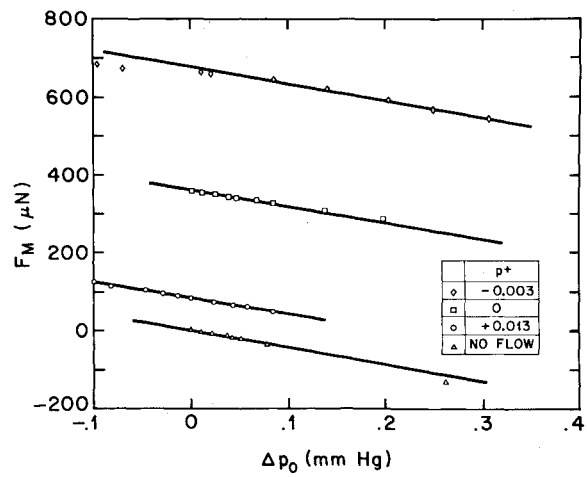

Fig. 7 Influence of pressure difference Δp_0 on indicated force F_M.

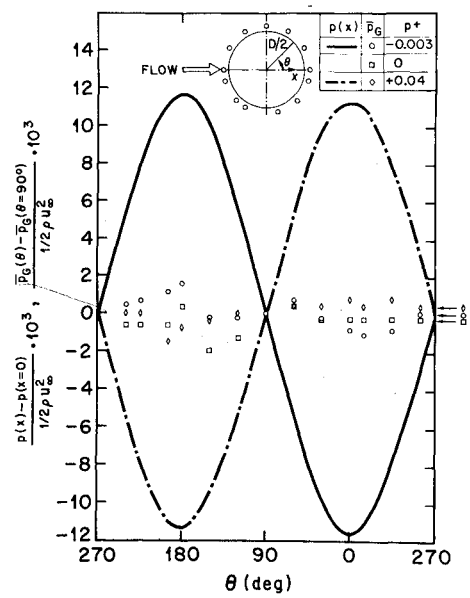

Fig. 8 Nondimensional distribution of static pressure $p_G(z,\theta)$ around element, together with corresponding variation of streamwise pressure. Sketch shows locations of pressure taps around circumference. Arrows indicate levels of p_H for the different data.

force which agree to better than 5% with values obtained from Preston-tube measurements (the latter agree to within 3% with those obtained from velocity profiles using the Clauser chart).

Initial tests showed that the floating-element instrument is extremely sensitive to a nonuniform protrusion or recession of the element in the measuring surface. Such a tilt can be minimized in an iterative manner using the differential adjustment screws as follows. After adjustment of a differential screw, the magnitude of the shear force was measured first with the instrument mounted in the usual way, and then rotated through 180 deg relative to the flow direction. The process was repeated until the two values agreed to within the resolution of the instrument (a few micronewtons). The comparisons shown in Fig. 5 were made after these adjustments, and the alignments held unchanged for later measurements with streamwise pressure gradients. Experience has indicated that this dynamic alignment procedure led to more reliable results than an adjustment based solely upon an optically detectable misalignment.

The differential adjustment screws also allow the element to be raised or lowered with respect to the baseplate, thereby permitting investigation of the influence of a uniform protrusion or depression z of the element. The results given in Fig. 6 are are consistent with those of Allen[9] who also found almost central symmetry, although the range of values presented herein for z/δ is much smaller than his (about ± 0.002 compared with ± 0.017). The corresponding values of z^+ are 4.5, 3.0, and 1.3 for the favorable, zero, and adverse pressure gradient cases, respectively. Since it is quite straightforward to reduce the misalignment to less than 10 μm ($z/\delta \cong 0.0004$), the experiments presented herein cover the range of practical interest, and it is evident that the effect of a protrusion or recession of this magnitude is measurable but small.

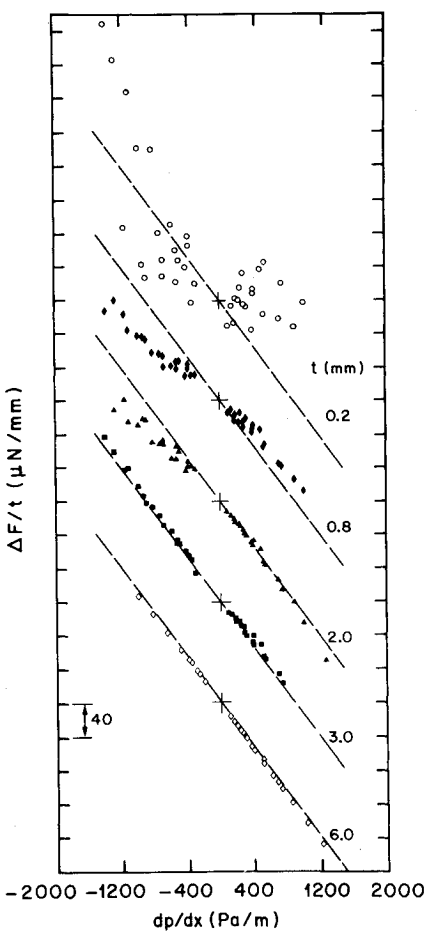

Fig. 9 Variation of $\Delta F/t$ with pressure gradient (symbols are the same as for Fig. 5).

Pressure Gradient Tests; Gap Flow

The crucial aspect of the pressure gradient tests was to systematically investigate the buoyancy force. Initial tests conducted with instruments 1 and 2 confirmed an approximately linear variation of the buoyancy force with dp/dx, but indicated different values of f for $p^+ > 0$ and $p^+ < 0$. This inconsistency motivated a series of tests to examine in greater detail the influence of flow through the gap, which Brown and Joubert suggested was likely to be of dominating influence as far as the secondary forces were concerned. First, Δp_0 was varied as in the determination of x_0, but to levels that would result in unidirectional flow through the gap in the presence of an external flow. The results for zero, positive, and negative pressure gradient are given in Fig. 7 for instrument 2. In each case the variation of F_M closely parallels the no-flow results, suggesting that there can be no significant disturbance to the boundary layer for values of Δp_0 close to zero (as is the case in actual operation of the instrument). Furthermore, visualization (for $p^+ > 0$) using smoke failed to reveal any motion within the housing suggesting that any gap flow must be of a very low volume.

As a further check on the possible influence of a gap flow, profiles of mean velocity and longitudinal turbulence intensity were measured using a hot-wire probe at the center of the element and also directly over the gap on either side. These measurements indicated that any disturbance due to the presence of the floating element is limited to a slight increase in the degree of scatter in the velocity measurements and turbulence level, but that there is no significant shift in the velocity profile (which would correspond to a change in τ_s). Both checks suggest that the gap flow is insufficient to disturb the external boundary layer.

As a next step, the angular distribution of gap pressure $p_G(\bar{z},\theta)$ was measured using 13 pressure taps drilled in the lip of the baseplate of instrument 2, $\bar{z}$ indicating that the measurement made represents an average over some fraction of the lip thickness: the taps are 0.5 mm in diameter and located within the gap so as to be symmetric with respect to the element thickness. The measurements in Fig. 8 show that for both positive and negative pressure gradients p_G is effectively constant and equal to the housing pressure p_H and so indicate that the change in pressure from the external value to p_H must take place over a very small fraction of the element

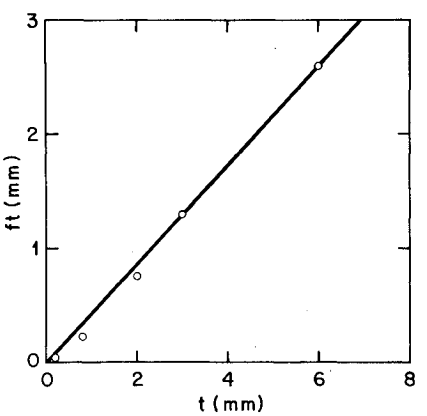

Fig. 10 Variation of ft with t.

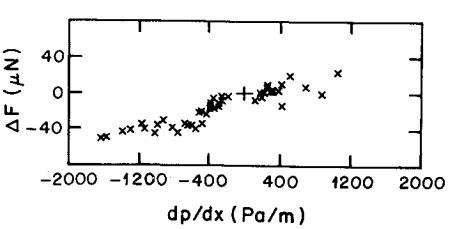

Fig. 11 Dependence of buoyancy force ΔF on pressure gradient for instrument 3 ($t/g = 0.4$).

lip, rather than in the linear variation that would result in a value of $f=0.5$.

Effect of Varying Lip Thickness

The tests described previously did not reveal any evidence of local flow distortion in the vicinity of the gap that could have influenced the floating-element measurement, and the inconsistent behavior observed in positive and negative pressure gradients remained unexplained. An attempt to understand the influence of gap geometry on the flow and resultant pressure distribution in the gap motivated the testing of a series of floating elements with different lip thicknesses. These elements, designated by numbers 3 through 8 in Table 1, with t varying from 0.02 to 6 mm, span a range in nominal t/g values from 0.4 to 100. For each of these elements the buoyancy force ΔF was determined over a range of pressure gradients. The results are given in Fig. 9 for all elements except that with $t=0.02$ mm in the form $\Delta F/t$ vs dp/dx and again confirm an approximately linear relationship. For sufficiently large t/g the data lead to the value 0.43 for f, suggesting that the gap pressure distribution is then independent of gap geometry but not linear. The reference lines in Fig. 9 correspond to this value for f, while values of ft for the individual elements are shown in Fig. 10. It may be remarked that as the thickness t is decreased, the scatter in the data increases, a trend which is probably attributable to two factors: an increasing sensitivity to alignment errors and the fact that the gap pressure distribution is no longer independent of the geometry. As is shown in Fig. 11, the behavior of element 3, for which $t=0.02$ mm, is totally inconsistent with the other instruments and leads to $ft<0$, suggesting that a sharp-edged element is not as desirable as it might seem at first.

In assessing the consequences of these experiments, it is important to bear in mind that since the buoyancy force scales with ft, it is desirable to have an instrument for which this quantity is as small as possible. On the other hand, it is still important to have a reliable estimate for f, which is realized more easily for the larger values of t (and ft). Evidently a compromise must be sought, and for the authors' design this would seem to be for $t\cong 2$ mm. Since the last two terms in Eq. (1), which together represent the net effect of a pressure gradient, are always of opposite sign, in principle, it is possible to eliminate the effect of a pressure gradient by choosing an appropriate element thickness (1.64 mm for $f=0.43$). Since the value of f is less well defined for smaller thicknesses, in practice a trial and error approach would be necessary to obtain the appropriate element thickness. A reconsideration of the problems encountered with elements 1 and 2, where different values of ft were found for $dp/dx<0$ and $dp/dx>0$, suggests that the discrepancies were due to a low value for t/g and the increased sensitivity to misalignment errors for both small gap sizes and small thicknesses.

Everett,[12] in assessing the effects of pressure gradient, covered values of t/g between 1.3 and 4.2, which are at the low end of the range of the present experiments. The values of the lip-force coefficient f extracted from his data varied between 0.55 and 1.32, so that his contention that the pressure variation across the lip is effectively linear and a value of $f=0.5$ is adequate in the pressure gradient correction for his elements is not really substantiated by his data. Nevertheless, the work presented herein confirms his conclusions.

With the value for f specified above, the residual error

$$\epsilon=\Delta F-ft\frac{dp}{dx}\frac{\pi D^2}{4}$$

was computed for all of the measurements. For $F_\tau>300$ μN this error is less than 5%, which is comparable with the results achieved by Brown and Joubert[11] and also with the uncertainties inherent in using the Preston tube.

Concluding Remarks

For the most part, the authors' conclusions are in general agreement with those based upon the earlier work cited. While direct evidence of the existence of gap flows could not be found, a systematic investigation of elements with different lip thicknesses confirmed that the net lip, or buoyancy, force resulting from nonuniformity of the pressure within the gap is the principal source of uncertainty in the use of a floating-element instrument in a flow with a nonzero external pressure gradient. With Preston-tube measurements taken as the standard for comparison, it is shown that the buoyancy force is roughly proportional to $t dp/dx$, and the limitations imposed by gap geometry on a simple model for this force are discussed. It is also concluded that the effects of protrusion or depression of the element can be reduced to a negligible level. All other forces acting on the element, with the exception of those due to the surface shear stress itself, are readily estimated.

Acknowledgments

The mechanical design was made by H. R. Grauwiller and the instruments were built by R. Graf, both of the Brown Boveri Research Center.

References

[1] Clauser, F. H., "Turbulent Boundary Layers in Adverse Pressure Gradients," *Journal of the Aeronautical Sciences*, Vol. 21, Feb. 1954, pp. 91-108.

[2] Acharya, M. and Escudier, M. P., "Measurements of the Wall Shear Stress in Boundary Layer Flows," *Proceedings of the Fourth Symposium on Turbulent Shear Flows*, Karlsruhe, FRG, Sept. 1983, pp. 277-286.

[3] Winter, K. G., "An Outline of the Techniques Available for the Measurement of Skin Friction in Turbulent Boundary Layers," *Progress in Aerospace Sciences*, Vol. 18, 1977, pp. 1-57.

[4] Schetz, J. A. and Nerney, B., "Turbulent Boundary Layer with Injection and Surface Roughness," *AIAA Journal*, Vol. 15, Sept. 1977, pp. 1288-1294.

[5] Voisinet, R. L. P., "Influence of Roughness and Blowing on Compressible Turbulent Boundary Layer Flow," U. S. Naval Surface Weapons Center, Silver Spring, Md., NSWC TR 79-153, June 1979.

[6] Karlsson, R. I., "Studies of Skin Friction in Turbulent Boundary Layers on Smooth and Rough Walls," Ph.D. Thesis, Department of Applied Thermo- and Fluid Dynamics, Chalmers University of Technology, Göteborg, Sweden, 1980.

[7] Frei, D. and Thomann, H., "Direct Measurements of Skin Friction in a Turbulent Boundary Layer with a Strong Adverse Pressure Gradient," *Journal of Fluid Mechanics*, Vol. 101, Pt. 1, Nov. 1980, pp. 79-95.

[8] Tennant, M. H., Pierce, F. J., and McAllister, J. E., "An Omnidirectional Wall Shear Meter," *Journal of Fluids Engineering*, Vol. 102, March 1980, pp. 21-25.

[9] Allen, J. M., "Experimental Study of Error Sources in Skin-Friction Balance Measurements," *Journal of Fluids Engineering*, Vol. 99, March 1977, pp. 197-204.

[10] Allen, J. M., "Improved Sensing Element for Skin-Friction Balance Measurements," *AIAA Journal*, Vol. 18, Nov. 1980, pp. 1342-1345.

[11] Brown, K. C. and Joubert, P. N., "The Measurement of Skin Friction in Turbulent Boundary Layers with Adverse Pressure Gradients," *Journal of Fluid Mechanics*, Vol. 35, Pt. 4, March 1969, pp. 737-757.

[12] Everett, H. U., "Calibration of Skin-Friction Balance Discs for Pressure Gradient," University of Texas, Defence Research Laboratory, Austin, Tex., DRL-426, Aug. 1958.

[13] Coles, D. E., "Measurements in the Boundary Layer on a Smooth Flat Plate in Supersonic Flow," Thesis, Jet Propulstion Laboratory, California Institute of Technology, Pasadena, Calif., May 1953.

[14] Bradshaw, P., "Two More Wind Tunnels Driven by Aerofoil-Type Centrifugal Blowers," Imperial College, London, Aero Rept. 71-10, 1972.

[15] Patel, V. C., "Calibration of the Preston Tube and Limitations on its Use in Pressure Gradients," *Journal of Fluid Mechanics*, Vol. 23, Pt. 1, Sept. 1965, pp. 185-208.